Al-Khwarizmi Engineering Journal, Vol. 5, No. 3 PP 16 - 22 (2009)

Al-Khwarizmi Engineering Journal

Analysis of Wave Propagation in Detection of Aorta Dieses Using Lumps Analysis

A. M Al-Jumaily* **A. Salam Al-Ammri****

* *Institute of Biomedical Technology / Auckland University of Technology/ Auckland, NZ*
ahmed.al-jumaily@aut.ac.nz

** *Department of Mechatronics Engineering/ Al-Khwarizmi College of Engineering/ University of Baghdad*
asalamalammri@yahoo.com

(Received 3 May 2009; accepted 6 August 2009)

Abstract

In this paper a theoretical attempt is made to determine whether changes in the aorta diameter at different location along the aorta can be detected by brachial artery measurement. The aorta is divided into six main parts, each part with 4 lumps of 0.018m length. It is assumed that a desired section of the aorta has a radius change of 100,200, 500%. The results show that there is a significant change for part 2 (lumps 5-8) from the other parts. This indicates that the nearest position to the artery gives the significant change in the artery wave pressure while other parts of the aorta have a small effect.

Keywords: *Wave propagation, aorta, lumps analysis.*

1. Introduction

Several cardiovascular pathologies introduce variation in the radius and thickness of the aorta. Plaques can cause severe arterial stenosis that leads to blood flow obstruction. The formation of fat deposits inside the aorta decreases the diameter and hinders, or even stops, the flow of blood. Also, excessive artery enlargements caused by atherosclerosis can lead to aneurysms and its rupture may lead to the sudden death. All these variations affect the pattern of pressure waves.

Kevin P.C[1] extracted clinically useful information from the shape of the diastolic portion of the blood pressure. A simple third order, lumped parameter circuit model was proposed to characterize the wave shape change in terms of the mechanical features of the systemic arterial system. Wen-shan Duan, etal.[2] proposed an approach to understand the effect of arterial branching in large arteries. Reflected and transmitted nonlinear waves at the arterial branching are analytically constructed from incident waves. JM Padilla1,etal.[3] evaluated the relationship among blood pressure parameters and abPWV, and the relationship among abPWV, SIDVP and RIDVP in health subjects. Aortic arterial stiffness is an independent predictor of cardiovascular risk. Pulse wave velocity (PWV) is the most validated and universally accepted measure of arterial stiffness. The Digital Volume Pulse (DVP) is an accurate and non-invasive method to obtain information on the pressure pulse waveform, and it provides two indexes: stiffness index (SIDVP) which relates with large artery stiffness, and the reflection index (RIDVP) which relates with vascular tone. SIDVP has been previously correlated with cfPWV (carotid-femoral PWV), however, the inguinal location of the employed transducer provokes a strong psychological impact on the patients, which may reduce reproducibility. By contrast, measurement of abPWV (ankle-brachial pulse wave velocity) minimizes this psychological stress. Temesgen Markos Kindo[4] measured the size of an aneurysm as the indicator of rupture potential and the necessity of medical intervention; the larger the aneurysm is the higher the risk of rupture is. It

was observed that some large aneurysms stayed intact whereas smaller ones ruptured. Kamran Hassani etal.[6] showed that the decreasing of pressure along the aorta and renal artery lengths was due to the aneurysms and stenosis at the peak systole. The mathematical method demonstrated that compliances of the aorta sections and renal increased with the expansion rate of the aneurysms and stenosis. The results of the modelling, such as electrical pressure graphs, exhibited the features of the pathologies such as hypertension and were compared with the relevant experimental data.

Yannis Papaharilaou[7] assessed the merit of a decoupled fluid structure analysis of AAA wall stress. Anatomically correct patient specific AAA wall models were created by 3D reconstruction of computed tomography (CT) images. Flow simulations were carried out with inflow and outflow boundary conditions obtained from patient extracted data. Bedzinski [8] appointed experimentally the mechanical properties of abdominal aortic aneurysm (AAA) and abdominal aorta without pathological changes (NAA), in both directions: longitudinal (NAAl, AAAl) and circumferential (NAAc, AAAc). The investigations included the analysis of the stress - strain relationships of abdominal aortic aneurysm walls and unchanged abdominal aortas' walls, as well as estimation of the relationships between them. R. Cowling and J. Soria [9] investigated the flow characteristics in Abdominal Aortic Aneurysms using Planar Laser Induced Fluorescence (PLIF) for both steady and pulsatile flow conditions. For the pulsatile flow investigations a simple artificial waveform was used. Under steady flow conditions two zones were identified; the first one is the bulk fluid through the core of the expansion, and the second one is a recirculation zone occupying the majority of the expansion. M. Scotti [10] assessed the significance of assuming an arbitrary estimated peak fluid pressure inside the aneurysm sac for the evaluation of AAA wall mechanics, as compared with the non-uniform pressure resulting from a coupled fluid–structure interaction (FSI) analysis. In addition, a finite element approach was utilised to estimate the effects of asymmetry and wall thickness on the wall stress and fluid dynamics of ten idealised AAA models and one non-aneurysmal control. The results showed that the inclusion of fluid flow yields a maximum AAA wall stress up to 20% higher than that which is obtained with a static wall stress analysis with an assumed peak luminal pressure of 117 mmHg.

José F.[11] studied the influence of geometry and material anisotropy on the magnitude and distribution of the peak wall stress in AAAs. Three dimensional computer models of symmetric and asymmetric AAAs were generated in which the maximum diameter and length of the aneurysm were individually controlled. They show a strong influence of the material anisotropy on the magnitude and distribution of the peak stress. Results confirm that the relative aneurysm length and the degree of aneurismal asymmetry should be considered in a rupture risk decision criterion for AAAs. Peter C[12] showed that larger aneurysms increased risk of rupture because 1) they experience greater circumferential wall stress tending to expand the lumen, and 2) they are less distensible with a higher elastic modulus which indicates they have less reserve stretch capacity.

2. lumps Analysis

Mathematical analysis leads to greater understanding and improving the diagnosis and treatment of cardiovascular diseases. This study is based on the work proposed by A.M Al-Jumaily and Essa El-Aklouk[13]. They developed a mathematical formulation to describe pressure wave propagations, reflection in elastic branching arteries and the transmission of pressure from the brachial artery through the arm soft tissue to the pneumatic cuff Fig.(1).

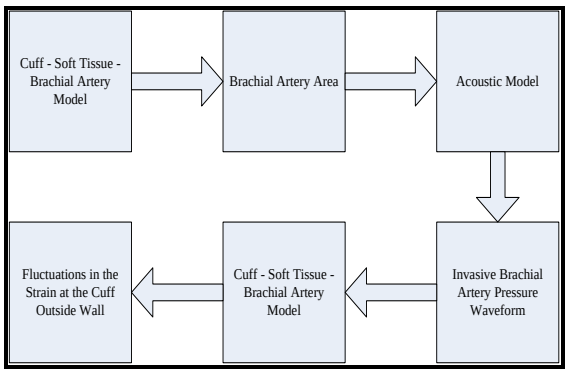

Fig. 1. Flow Chart of The Acoustic Model and the Cuff-Soft Tissue-Brachial Artery Model[13].

The material properties and geometry for the cuff, arm soft tissue, and the brachial artery used were adopted from the values reported by Muriso et al [14-16]. The number of lumps that would accurately describe the wave propagation in the arteries is conducted from the experiment data of

Westerhof et al [17]. The aorta was divided into 24 lumps of 0.018m length each while the subclavian and brachial arteries were divided into 16 lumps of 0.026m length each and the systolic cuff pressure was 120 mmHg. Figures (2& 3) give the variation in thickness and radius of the aorta, and the subclavian-brachial arteries.

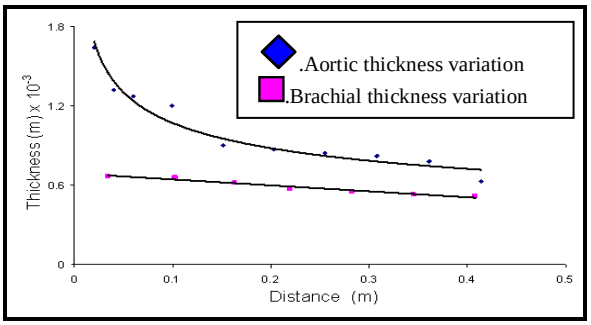

Fig. 2. The Human Aorta and the Subclavian and Brachial Arteries. Thickness Variation[17].

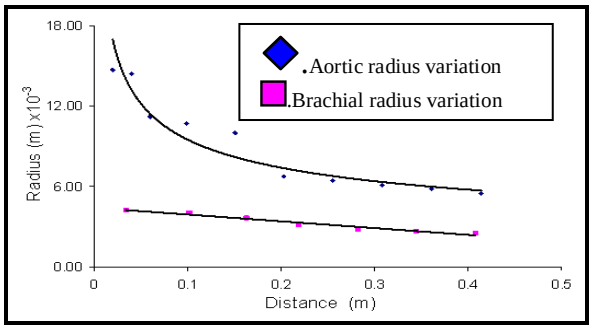

Fig. 3. The Human Aorta and the Subclavian and Brachial Arteries Radius Variations. [17].

Four feature points were extracted from the pressure contours to measure aortic stiffness. These feature points are (t1,t2) the time duration before the deflection marking the arrival of the incident and reflected waves respectively and (P1,P2) the peak of the first and second pressure deflection minus the diastolic pressure. The radial AI is used as an indicator for aortic stiffening and can be written as:

$$AI = P2 / P1$$

And the Time Lag is written as:

$$Time\ Lag = t2 - t1$$

The pressure contour has the same shape and contains all the feature points found in invasively measured brachial artery contours Fig.(4).

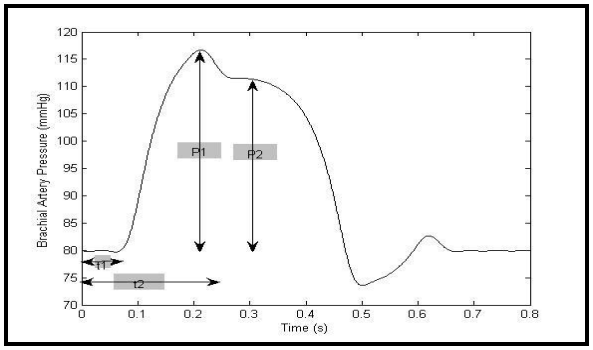

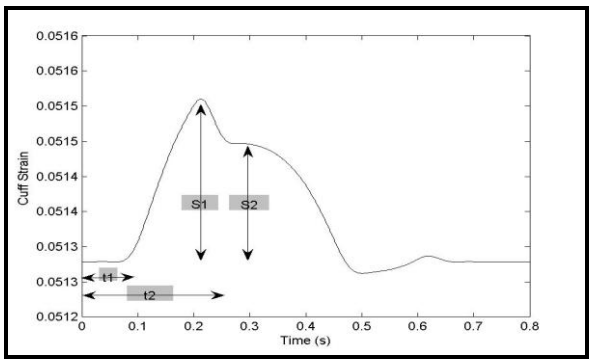

Fig. 4. Brachial Artery Pressure Waveform for a Healthy Young Adult. [13].

3. Results and Discussion

The effect of changing the aorta radius on the brachial artery pressure waveform and the strain on the external wall of the pneumatic cuff ranging from a healthy aortic stiffness (100%) to a diseased/aged aortic stiffness (200% and 500%) was shown in Figures 2&3. To extract clinical useful information, the aorta is divided into six main parts, each part with 4 lumps.The radius of each part increased by 100%, 200%, 500% and keeping the radius of other parts unchanged. All other model parameters were kept constant.

It is found that the increasing of radius by 200% will change the stiffness index by 1.2% for the first part (lumps 1-4), 5.5 % for the second part (lumps 5-8) and 1.8% for other parts of the aorta, while increasing the radius by 500 % will change the stiffness index by 3.35 for the first part, 10% for the second part and 4.6% for the other parts. The increasing of radius by 200% will change the time lag by 1.6% for the first part, 13 % for the second part and 3.3% for other parts, while increasing the radius by 500 % will change the time lag by 9.8% for the first part, 42.6% for the second part and 26% for the other parts. The strain on the pneumatic cuff outer wall

contour in Figure 6 shows the main change for part 2 (lumps 5-8) of the aorta from the other parts.

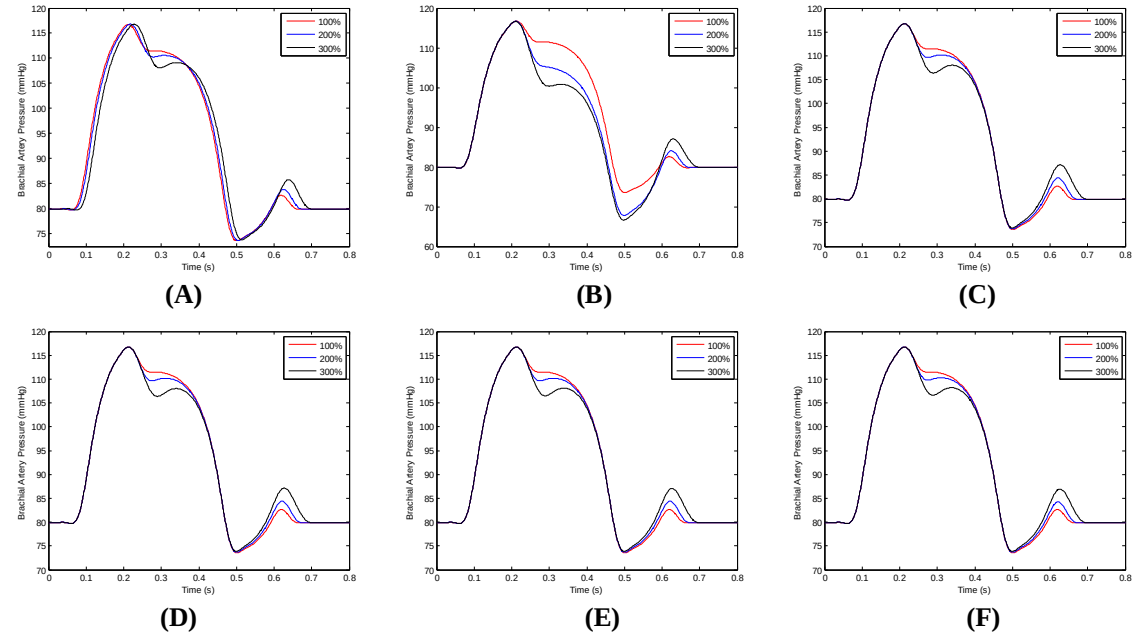

Fig. 5. Brachial Artery Pressure Waveforms at Different Part Aortic Radius for Percent 100, 200 500, %, [A:1-4,B:5-8,C:9-12,D:13-16,E:17-20,F:21-24 Lumps]

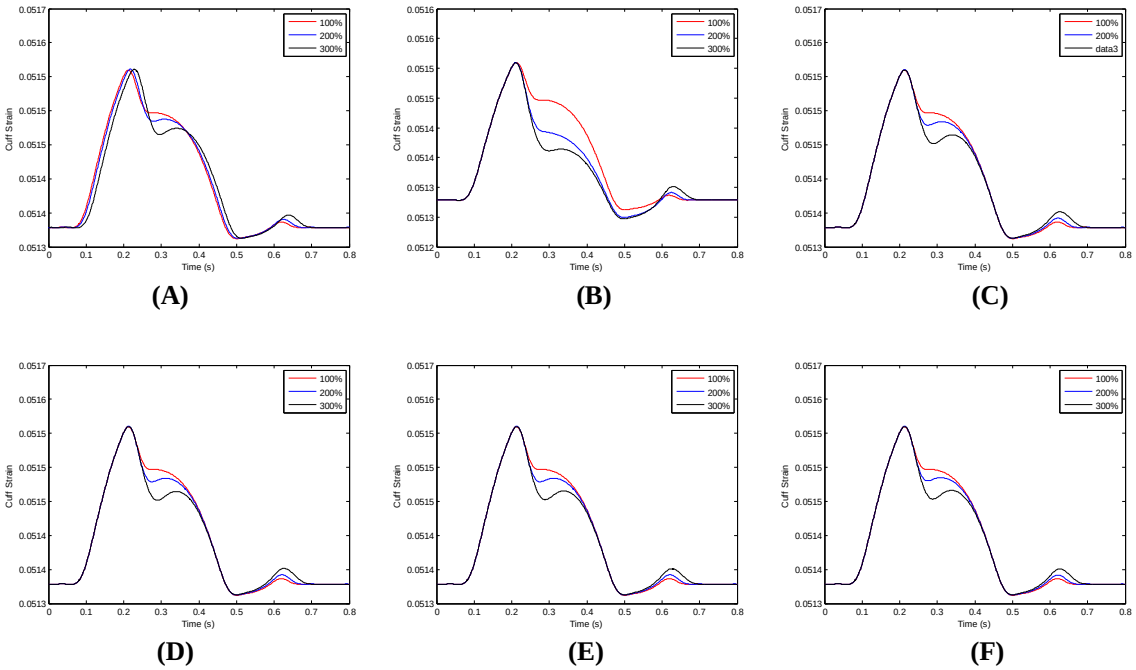

Fig. 6. Strain on the Pneumatic Cuff Outer Wall Contours at Different Part Aortic Radius for Percent 100, 200 ,500% , [A:1-4,B:5-8,C:9-12,D:13-16,E:17-20,F:21-24 Lumps].

Table 1,
Showing the Effect of Aortic Radius on the Feature Points of the Brachial Artery Pressure Contours, (AI_p), and Time Lag.

Radius %	Part (lumps)	P1 mmHg	P2 mmHg	AI%	t1 (s)	t2 (s)	Time Lag (s)	Mean	Median	Mode	Std	Range
100%	1-4	116.7	111.5	95.5	.213	.274	.061	91.98	82.26	73.55	15.03	43.17
	5-8	116.7	111.5	95.5	.213	.274	.061	91.98	82.26	73.55	15.03	43.17
	9-12	116.7	111.5	95.5	.213	.274	.061	91.98	82.26	73.55	15.03	43.17
	13-16	116.7	111.5	95.5	.213	.274	.061	91.98	82.26	73.55	15.03	43.17
	17-20	116.7	111.5	95.5	.213	.274	.061	91.98	82.26	73.55	15.03	43.17
	21-24	116.7	111.5	95.5	.213	.274	.061	91.98	82.26	73.55	15.03	43.17
200%	1-4	116.8	110.2	94.3	.218	.28	.062	91.98	83.17	79.91	14.81	43.19
	5-8	116.7	105.4	90.3	.211	.28	.069	89.6	82.55	79.92	14.5	48.89
	9-12	116.8	109.6	93.8	.213	.276	.063	91.98	83.61	79.9	14.67	43.06
	13-16	116.7	109.6	93.8	.213	.276	.063	91.98	83.61	79.9	14.67	43.06
	17-20	116.8	109.6	93.8	.213	.274	.063	91.98	83.61	79.9	14.67	43.06
	21-24	116.8	109.8	93.8	.213	.274	.063	91.98	83.5	73.59	14.7	43.07
500%	1-4	116.8	108.1	92.5	.229	.296	.067	91.98	84.66	79.9	14.39	43.03
	5-8	116.8	100.3	85.8	.212	.299	.087	89.07	84.4	66.65	13.99	50.02
	9-12	116.8	106.4	91.1	.213	.29	.077	91.98	85.73	79.9	14.03	42.84
	13-16	116.8	106.4	91.1	.213	.29	.077	91.98	85.73	79.9	14.03	42.84
	17-20	116.8	106.4	91.1	.213	.29	.077	91.98	85.68	73.88	14.05	42.85
	21-24	116.8	106.4	91.1	.213	.289	.076	91.98	85.68	73.88	14.05	42.85

4. Conclusion

The results show that the increase of radius will decrease the stiffness index and increase the time lag**.** It is found that there is a significant change brachial artery pressure waveforms and strain on the pneumatic cuff outer wall contours for part 2 (lumps 5-8) of the aorta from the other parts. The main changes are found in P2, t2 as indicated in figure 2 and table 1. The same conclusion is for S2 and t2 as shown in Figure 3. The statistical parameters, the mean and range could be used as another good indication for these changes. This indicates that the nearest position of changing the radius to the artery gives the significant change in the artery wave pressure while other parts of the aorta have a small effect.

Acknowledgments

We gratefully acknowledge the facilitated of IBTec, AUT University, NZ for using and modifying Essa El-Aklouk computer program

5. References

[1] P.C Kevin, ”Extracting new information from the shape of the blood pressure pulse”, Massachusetts institute of technology, February 1990

[2] Wen-shan Duan, Ben-ren Wang, and Rong-jue Wei1,”Reflection and transmission of nonlinear blood waves due to arterial branching”, Physical Review E Volume 55,Number 2 February 1997.

[3] JM Padilla1,2, EJ Berjano1, J Sáiz1, L Fácila3,P Díaz4, S Mercé4 "Assessment of Relationships between Blood Pressure, Pulse Wave Velocity and Digital Volume Pulse ",Computers in Cardiology 2006;33:893−896.

[4] Temesgen Markos Kindo "Mechanical Degradation and Remodelling of Cerebral Arteries", Technische University Eindhoven ,Eindhoven, October 2006

[5] José F. Rodríguez1 ,Cristina Ruiz,Manuel Doblaré, "Mechanical Stresses in Abdominal Aortic Aneurysms: Influence of Diameter, Asymmetry, and Material Anisotropy", Journal of Biomechanical Engineering Copyright © 2008 by ASME APRIL 2008, Vol. 130 / 021023-

[6] Kamran Hassani, Mahdi Navidbakhsh , Mostafa Rostami," Modelling of the aorta artery aneurysms and renal artery stenosis using cardiovascular electronic system", BioMedical Engineering Online 2007, **6**:22 doi:10.1186/1475-925X-6-22

[7] Yannis Papaharilaou, John A. Ekaterinaris, Eirini Manousaki, Asterios N. Katsamouris ,"Stress Analysis In Abdominal Aortic Aneurysms Applying Flow Induced Wall Pressure",5th GRACM International Congress on Computational Mechanics Limassol, 29 June – 1 July, 2005

[8] R. Bedzinski.□, M. Kobielarz M.S.□, S. Szotek, Ph.D.□, J. Filipiak, Ph.D. □, J. Janusz Gnus M.D.□ □, W.Hauser M.,"Directional Mechanical Properties of Abdominal Aorta-in Vitro Study",22nd ANUBIA-ADRIA Symposium on Experimental Methods in Solid Mechanics,September 28 - October 1, 2005 ,MONTICELLI TERME / PARMA - ITALY

[9] R. Cowling and J. Soria ,"Flow Visualisation through Model Abdominal Aortic Aneurysm", Fourth Australian Conference on Laser Diagnostics in Fluid Mechanics and Combustion ,The University of Adelaide, South Australia, Australia 7-9 ,December 2005

[10] M. Scottia,Christine Jorge Jimenezb, Satish C. Mulukc and Ender A. Finola,d,"Wall stress and flow dynamics in abdominal aortic aneurysms: finite element analysis vs.fluid–structure interaction",Computer Methods in Biomechanics and Biomedical Engineering Vol. 11, No. 3, June 2008, 301–322 ,Mona Abdolrazaghi, Mehdi NavidBakhsh and Kamran Hassani

[11] F José. Rodríguez,Cristina Ruiz ,Manuel Doblaré ,Gerhard A. Holzapfel," Mechanical Stresses in Abdominal Aortic Aneurysms:Influence of Diameter,Asymmetry, and Material Anisotropy", Journal of Biomechanical Engineering Copyright © 2008 by ASME APRIL 2008, Vol. 130 / 021023-1

[12] Peter C. Lin,"Mechanical Properties of Aneurysms of the Descending Human Aorta",Yale University School of Medicine ,Doctor of Medicine,2007

[13] A.M. Al-Jumaily and Essa El-Aklouk," An investigation into the acoustic response of the arteries",Mphil thesis, Auckland University of Technology (AUT),Auckland,2007

[14] M. Ursino, , C. Cristalli, , 1995, Mathematical modeling of noninvasive blood pressure estimation techniques – part I- Pressure transmission across the arm tissue, ASME Journal of Biomechanical Engineering, 117:107-116.

[15] M. Ursino, Cristalli, C., 1995, Mathematical modeling of noninvasive blood pressure estimation techniques – part II- Brachial Hemodynamics, ASME Journal of Biomechanical Engineering, 117:117-126.

[16] M Ursino, Cristalli, C., 1996, A Mathematical Study of Some Biomechanical Factors Affecting the Oscillometric Blood Pressure Measurement, IEEE Transactions on Biomedical Engineering, 43:761-78.

[17] N Westerhof, Bosman, F., De Vries CJ., et al , 1969, Analog studies of human systemic arterial tree, Journal of biomechanics, 2:121-143.

تحليل تقدم الموجات في تشخيص أمراض الشريان الأبهر بوساطة تقسيمه الى عدة مناطق

احمد الجميلي * عبد السلام العامري**

** جامعة اوكلاند / نيوزلندة*

ahmed.al-jumaily@aut.ac.nz

*** قسم هندسة الميكاترونيكس/ هندسة الخوارزمي/ جامعة بغداد*

asalamalammri@yahoo.com

الخلاصة

تم في هذا البحث وضع دراسة نظرية لحساب تغير نصف القطر للشريان الأبهر في عدة مناطق وإمكانية تحسس هذا التأثير من خلال قياس الضغط و الإجهاد في شريان اليد . تم تقسيم الشريان الأبهر الى ستة أجزاء كل جزء مكون منستة مقاطع وكل مقطع يحتوي على أربعة أجزاءبطول 0.018 m . تم فرض أن في كل مقطع تحصل فيه زيادة في القطر 100%،200%، 500 % .لقد أظهرت النتائج بان هناك تأثير واضح لزيادة القطر في المقطع الثاني (5-8 جزء) من الزيادة في المقاطع الأخرى مما يدلل المنطقة القريبة من الشريان التي يحصل فيها الانتفاخ من منطقة القياس تعطي تأثيرا واضحا من الأجزاء الأخرى .